Bioorganic & Medicinal Chemistry xxx (2016) xxx–xxx

Contents lists available at ScienceDirect

Bioorganic & Medicinal Chemistry

journal homepage: www.elsevier.com/locate/bmc

Binding mode prediction of aplysiatoxin, a potent agonist of protein kinase C, through molecular simulation and structure–activity study on simplified analogs of the receptor-recognition domain

Yoshiki Ashida [a], Ryo C. Yanagita [b,*], Chise Takahashi [c], Yasuhiro Kawanami [b], Kazuhiro Irie [d]

[a] Department of Applied Bioresource Science, The United Graduate School of Agricultural Sciences, Ehime University (Kagawa University), Kagawa 761-0795, Japan
[b] Department of Applied Biological Science, Faculty of Agriculture, Kagawa University, Kagawa 761-0795, Japan
[c] Division of Applied Bioresource Science, Graduate School of Agriculture, Kagawa University, Kagawa 761-0795, Japan
[d] Division of Food Science and Biotechnology, Graduate School of Agriculture, Kyoto University, Kyoto 606-8502, Japan

ARTICLE INFO

Article history:
Received 13 June 2016
Revised 5 July 2016
Accepted 6 July 2016
Available online xxxx

Keywords:
Aplysiatoxin
Tumor promoter
Protein kinase C
Molecular dynamics simulation
Structure–activity study

ABSTRACT

Aplysiatoxin (ATX) is a naturally occurring tumor promoter isolated from a sea hare and cyanobacteria. ATX binds to, and activates, protein kinase C (PKC) isozymes and shows anti-proliferative activity against human cancer cell lines. Recently, ATX has attracted attention as a lead compound for the development of novel anticancer drugs. In order to predict the binding mode between ATX and protein kinase Cδ (PKCδ) C1B domain, we carried out molecular docking simulation, atomistic molecular dynamics simulation in phospholipid membrane environment, and structure–activity study on a simple acyclic analog of ATX. These studies provided the binding model where the carbonyl group at position 27, the hydroxyl group at position 30, and the phenolic hydroxyl group at position 20 of ATX were involved in intermolecular hydrogen bonding with the PKCδ C1B domain, which would be useful for the rational design of ATX derivatives as anticancer lead compounds.

1. Introduction

Aplysiatoxin (ATX, Fig. 1) is a polyacetate isolated from sea hare *Stylocheilus longicauda*[1] and cyanobacteria.[2] ATX showed potent tumor-promoting activity in vivo,[3] but also showed anti-proliferative activity against several human cancer cell lines.[4] The main cellular target of ATX is protein kinase C (PKC),[5] which is a serine/threonine kinase family that plays important roles in cellular signal transduction such as proliferation, differentiation, and apoptosis.[6] ATX binds to tandem C1 domains (C1A and C1B) of eight isozymes of conventional PKC (α, βI, βII, γ) and novel PKC (δ, ε, η, θ), resulting in translocation of these isozymes to the cellular membrane fraction to activate the enzymes (Fig. 2).[7]

Recently, ATX has attracted attention as a lead compound for the development of novel anticancer drugs targeting PKC isozymes.[8] While ATX and debromoaplysiatoxin (DAT) showed both anti-proliferative and tumor-promoting activities, their simplified analogs showed anti-proliferative activity comparable to DAT but showed little tumor-promoting activity.[9] Knowledge about the precise binding mode of ATX and PKC C1 domains is needed to rationally design ATX derivatives as anticancer drugs. Although several groups have reported comparisons of pharmacophoric elements between ATX and other PKC ligands,[10,11] a precise binding mode of ATX with the PKC C1 domains has not yet been proposed.

Although X-ray crystallography and NMR-based methods are 'gold standards' for analysis of protein–ligand interaction and binding mode, it is difficult to apply these methods to the PKC ligand/C1 domain system because holo-C1 domain exists as a ternary complex of protein/ligand/phospholipid bilayer membrane.[12] To overcome this experimental limitation, we in the present study carried out molecular docking simulation, molecular dynamics simulation of ATX/C1 domain complex in phospholipid membrane environment, and structure–activity study on the receptor recognition domain of ATX.

Abbreviations: ATX, aplysiatoxin; PKC, protein kinase C; DAT, debromoaplysiatoxin; DAG, 1,2-diacyl-*sn*-glycerol; RD, recognition domain; MM, molecular mechanics; DFT, density functional theory; MD, molecular dynamics; POPS, 1-palmitoyl-2-oleoyl-phosphatidylserine; K_d, dissociation constant; K_i, binding inhibition constant.

* Corresponding author. Tel./fax: +81 87 891 3092.
E-mail address: charlesy@ag.kagawa-u.ac.jp (R.C. Yanagita).

http://dx.doi.org/10.1016/j.bmc.2016.07.011
0968-0896/

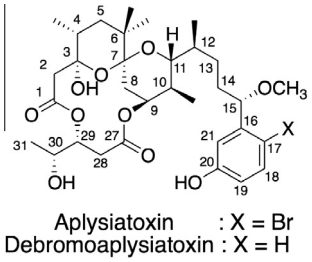

Figure 1. Structure of aplysiatoxins.

2. Results and discussion

2.1. Conformational search of ATX

ATX is composed of a 14-membered bis-macrolactone ring and a side chain containing an aromatic ring. In terms of receptor recognition and conformational control, the structure of ATX can be divided into three regions (Fig. 3):[13] the recognition domain (RD) at positions 1 and 27–31, the conformation-controlling unit from position 2 to 11, and the side chain at position 11. RD contains two ester groups and a hydroxyl group that could play some roles in the receptor recognition in a manner similar to those of an endogenous second messenger 1,2-diacyl-*sn*-glycerol (DAG).[10] The conformation-controlling unit contains a [6,6]-spiroketal moiety and is thought to keep RD in its active conformation.[10] Therefore, ATX can be viewed as a conformation-constrained analog of flexible DAG, whereas the direction of ester linkages at position 27 of ATX and *sn*-1 position of DAG are opposite. Finally, the side chain may play roles similar to those of hydrophobic part of naturally-occurring PKC activators such as phorbol esters (Fig. 3) and teleocidins.[11]

Although some protein–ligand docking programs can take into account flexibility of cyclic parts of a molecule in an indirect way, it may dramatically increase the number of rotatable bonds and computational complexity. Thus, prior to docking simulation, we performed conformational search for the macrolactone part of ATX.

Conformational search was carried out using simulated annealing (SA) method to generate 1000 geometries. The side chain at position 11 was replaced with an isopropyl group to simplify the calculation. The CHARMM general force field (CGenFF) was employed to calculate potential energy of the system. Among the

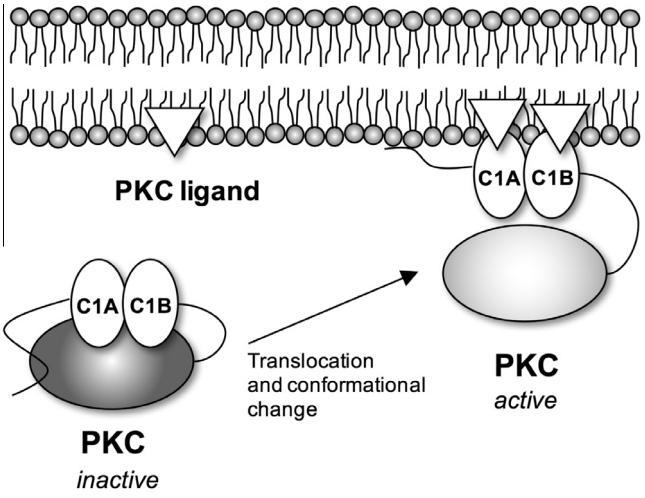

Figure 2. Activation mechanism of protein kinase C (PKC).

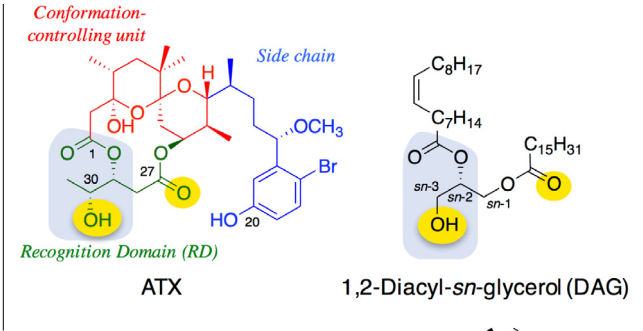

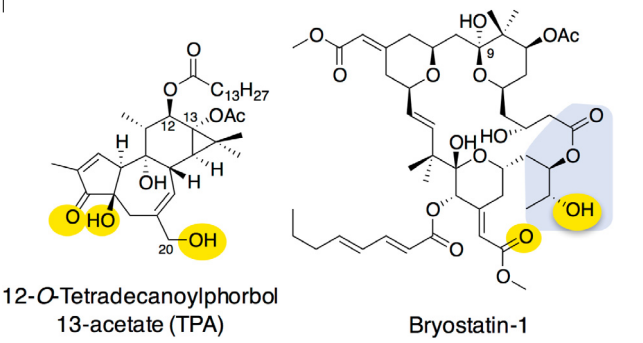

Figure 3. Structures and pharmacophoric elements of ATX, DAG, TPA, and bryostatin-1.

structures generated, 351 out of 1000 took chair–chair [6,6]-spiroketal conformation as with the experimental structures in solution and crystal.[14] They were classified into six groups (A–F) based on the lactone ring conformation. Table 1 lists size and average molecular mechanics (MM) energy of each group. While conformers B and C were identical to RD-I and RD-II conformers calculated by Knust and Hoffmann for 3-deoxyaplysiatoxin,[13] respectively, conformers A, D, E, and F were newly identified ones. Conformer A with the lowest energy was conformationally close to conformer B. Conformational difference between them was only orientation of the carbonyl group at position 27; the dihedral angle difference at C9–O9 was approximately 40 degrees (Fig. 4). Although average MM energies for conformers C and D were within 5 kcal/mol from that of conformer A, the 30-OH group in these conformers formed intramolecular hydrogen bonding with other parts of the molecule, lowering the potential energy of the conformers. However, this 30-OH group was predicted to form hydrogen bondings with the PKCδ C1B domain. Therefore, we considered that binding of conformers C and D to the PKC C1 domain is energetically unfavorable. Conformers E and F were poor in terms of either group size or energy. Since conformer B was almost identical to the crystal conformation (Fig. 4), we postulated that conformers A and/or B are active conformers. To estimate the relative stabilities of and energy barrier between conformers A and B, we performed density functional theory (DFT) calculations. The molecular geometry optimization of these conformers and

Table 1
Conformational analysis of macrocyclic core of ATX

Conformer	No. in cluster	Average MM energy (kcal mol^{-1})	Relative MM energy (kcal mol^{-1})
A	57	−127.61	0
B	167	−125.21	2.40
C	63	−123.44	4.17
D	55	−122.75	4.86
E	7	−122.41	5.20
F	1	−104.05	23.56

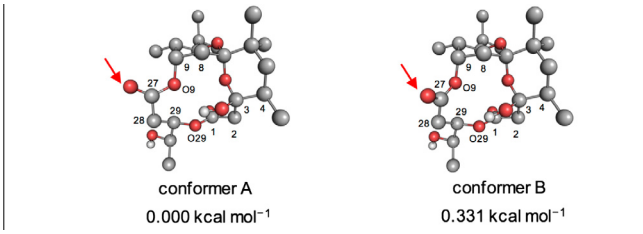

Conformer	dihedral angles (-180 < φ < +180)					
	9—O9	27—28	28—29	29—O29	1—2	2—3
A	+134°	−23°	+75°	−149°	−65°	−167°
B	+93°	+20°	+62°	−148°	−64°	−168°
Crystal structure of dibromo-ATX[a]	+107°	−3°	+73°	−142°	−58°	−167°

[a] Ref. 14.

Figure 4. Possible conformers of a macrocyclic core of ATX and their relative energy at the ωB97X-D/6-31G* level.

intermediate conformers between them was performed at the ωB97X-D/6-31G* level of theory. Figure 4 shows optimized geometries and relative energies of conformers A and B. The difference in energy between conformers A and B was 0.331 kcal·mol^{-1}, and energy barrier was only 0.602 kcal·mol^{-1}. The small energy difference and barrier indicate that these conformers readily interconvert with each other at room temperature and that the orientation of the carbonyl group at position 27 is not restricted to its local minima, conformers A and B.

2.2. Docking simulation of ATX with PKCδ C1B domain

Since the DFT calculation indicated that the difference in energy between conformers A and B is very small, we performed docking simulation of the both conformers with a crystal structure of PKCδ C1B domain (PDB code: 1PTR)[15] using the AutoDock[16] program (version 4.2.6). The macrolactone ring of ATX was treated as rigid, and the other parts of ATX and side chain of Leu-254 of the receptor were treated as flexible. From two hundred docking results for each conformer, binding modes where 30-OH group of the ligand forms hydrogen bonds with Thr-242 and Leu-251 of the receptor were selected as valid binding modes because the 30-OH group of ATX was postulated to play the same role as 20-OH group of phorbol esters that formed hydrogen bonds with the PKCδ C1B domain in the crystal structure (Fig. 3).[15] Three docking results were selected for both conformers, in all of which the carbonyl group at position 27 formed a hydrogen bond with the N–H group of Gly-253. This binding mode corresponds to the binding mode of DAG predicted by Marquez et al.[17] and Li et al.,[18] where the *sn*-1 carbonyl group of DAG formed a hydrogen bond with the Gly-253.

2.3. Molecular dynamics simulation of ATX/PKCδ C1B domain complex in phospholipid membrane environment

Next, we carried out molecular dynamics (MD) simulation of ATX/PKCδ C1B domain complex in phospholipid membrane environment to refine the binding model from the docking simulation. At first, ATX/PKCδ C1B domain complex was inserted into 1-palmitoyl-2-oleoyl-phosphatidylserine (POPS) bilayer membrane, then the system was equilibrated followed by 10 ns of production MD simulation. We chose phosphatidylserine (PS) as a lipid component because binding of the PKC ligands to the C1 domains shows specificity for PS.[19] The PKCδ C1B domain and the lipids were described by the charmm36 force field[20] with modification for zinc-coordinated structures. ATX was described by the CGenFF force filed (version 3.0.1), which could reproduce conformational energy landscape of ATX relatively well. During the 10 ns of the production run, root mean square deviation (RMSD) of backbone atoms of the protein and all atoms of the ligand from the initial structure remained at values below 2 and 1 Å (Supplemental Fig. S1), respectively, suggesting adequacy of the stability of the model.

Figure 5 shows an overview of the system (Fig. 5A), interactions between ATX/PKCδ C1B domain and the phospholipids (Fig. 5B), and the representative binding mode between ATX and the receptor (Fig. 5C). ATX and the hydrophobic residues forming the binding cleft were located in a hydrophobic core of the PS membrane and were fully dehydrated (Fig. 5A and B).

In the binding model (Fig. 5C), four hydrogen bonds were formed between ATX and δ-C1B: In addition to three hydrogen bonds observed in the docking simulation, a hydrogen bond between phenolic 20-OH group of ATX and C=O group of Met-239 was observed. This result is consistent with a report that 20-*O*-methyldebromoaplysiatoxin was less active in induction of mouse-ear irritation, induction of ornithine decarboxylase (ODC), and the inhibition of specific 12-*O*-tetradeconylphorbol 13-acetate (TPA) binding than in debromoaplysiatoxin (DAT).[21] The C=O group of Met-239 was also predicted to form a hydrogen bond with 9-OH group of bryostatin-1.[22] The average distances among these hydrogen-bonding pairs, r_{AH}, during the MD simulation are listed in Table 2. These distances can be categorized as moderate (1.5–2.2 Å) and weak (2.2–3.2 Å).[23] The standard deviation for these distances suggests that these hydrogen bonds were stably maintained during the simulation.

During the MD simulation, two conformations for the side chain at position 11 of ATX were observed, where dihedral angles for C11–C15 were T–T–T–G$^-$ or T–G$^+$–T–G$^+$ (T, *trans*; G, *gauche*; Fig. 6), though the hydrogen bond between the 20-OH of ATX and Met-239 was maintained in both conformations.

2.4. Molecular electrostatic potential calculation of ligand/PKCδ C1B domain complex

The MD simulation provided clear insights into the role of the 20-OH, 27-C=O, and 30-OH groups of ATX in the PKC binding. However, the ester group at position 1 was not involved in any intermolecular hydrogen bond with the receptor and its role remained unclear, despite its presence in three major classes of PKC activators: aplysiatoxins, DAG, and bryostatins (Fig. 3). In order to predict the role of the ester group at position 1, we focused on molecular electrostatic potentials of ATX and the receptor. Electrostatic potential complementarity as well as shape complementarity is a key determinant of molecular recognition.[24] Figure 7A shows electrostatic potential surface of the PKCδ C1B domain alone or in complex with phorbol 13-acetate (PDB code: 1PTR). A ligand binding cleft of the PKCδ C1B domain was characterized by a marked positive potential of the back wall and the bottom as well as neutral to negative potential of the left frontal part. As shown in Figure 7B, ATX had an electrostatic potential surface complementary to the binding cleft. The polarization of the ester group at position 1 of ATX could contribute to this complementary electrostatic potential. Moreover, we found that phorbol 13-acetate had a potential surface similar to that of ATX (Fig. 7C), supporting the predicted binding mode of ATX with the PKCδ C1B domain.

2.5. Synthesis and PKC binding of acyclic analogs of the recognition domain of ATX

Although the effect of modification of 20-OH and 30-OH groups of ATX on the PKC binding have been studied previously, the role of

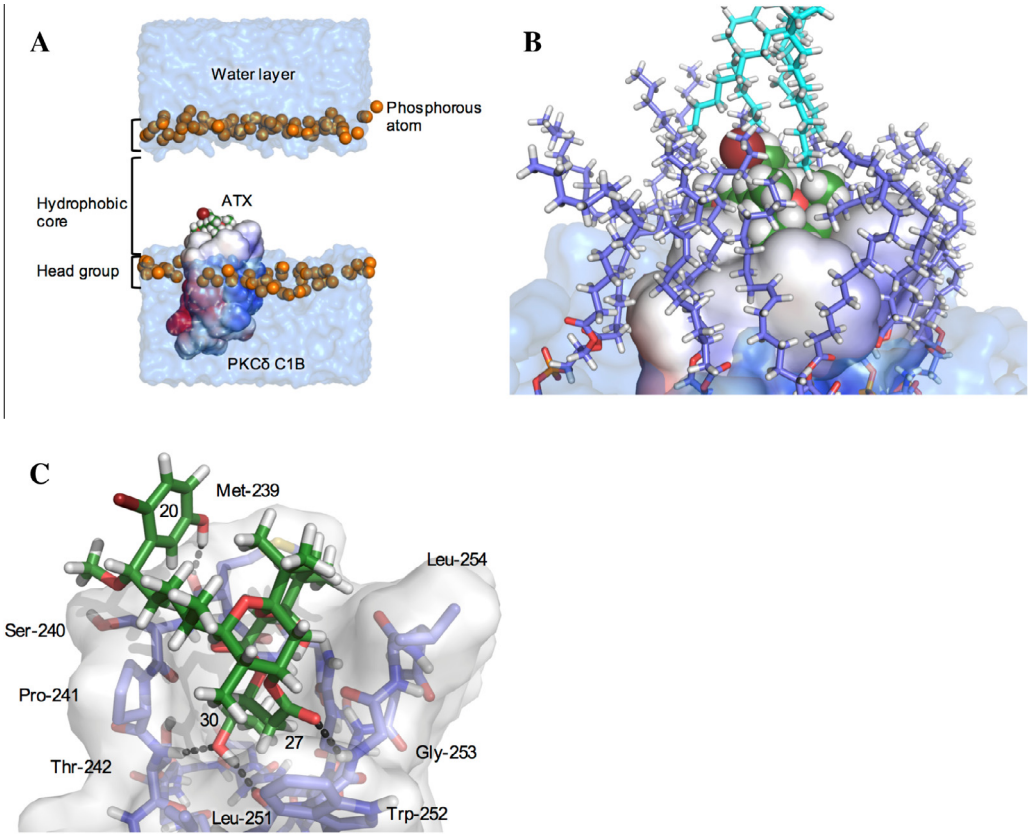

Figure 5. Structures of a ternary complex of POPS membrane/ATX/PKCδ C1B domain obtained from the MD simulation. (A) Overall structure of the POPS membrane/ATX/PKCδ C1B domain complex in water after the 10 ns of production run. Protein is depicted in surface; ATX is in spheres colored green (carbon), red (oxygen), firebrick red (bromine), and white (hydrogen); phosphorous atoms of the lipids are in spheres (orange); water layer is depicted as surface (blue). (B) Interaction between POPS and ATX/PKCδ C1B domain complex. ATX is in spheres and POPS are in stick model. The carbon atoms of POPS from upper and lower leaflet were colored by cyan and slate, respectively. (C) Front views of structure of ATX/PKCδ C1B domain complex. ATX is in the stick model. The residues near the ligand are represented in the stick model colored purple (carbon), red (oxygen), blue (nitrogen), and white (polar hydrogen) with the labels of their residue names, while other residues are shown only in backbone. Black dashed lines represent hydrogen bondings.

Table 2
Hydrogen-bonding parameters derived from MD simulation of the ATX/PKCδ C1B complex

H-bond donors	H-bond acceptors	r_{AH} (Å)[a]
20-O*H* (ATX)	C=*O* (Met-239)	1.86 (0.16)[b]
N*H* (Thr-242)	30-O*H* (ATX)	2.27 (0.24)
30-O*H* (ATX)	C=*O* (Leu-251)	1.91 (0.17)
N*H* (Gly-253)	27-C=*O* (ATX)	2.29 (0.38)

[a] Distance between an acceptor atom and a hydrogen atom.
[b] Standard deviations from 1000 trajectories.

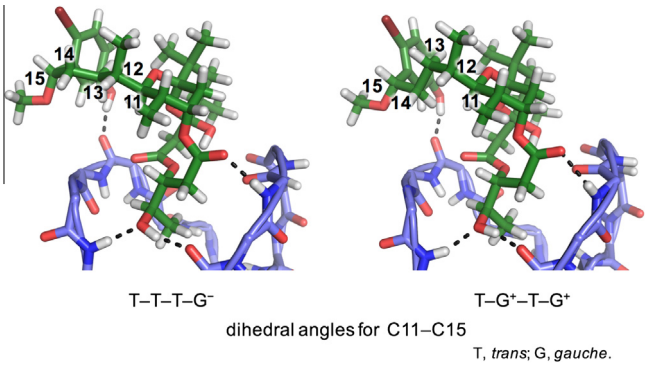

Figure 6. Two conformations of the side chain at position 11 of ATX during the MD simulation.

the two carbonyl groups in the recognition domain (RD) has not been experimentally examined. Thus, we examined the role of the carbonyl groups of ATX by employing ester-to-ethylene (–CH_2-CH_2–) and ester-to-ether modifications. In order to avoid possible conformational changes in the macrocyclic ring caused by these modifications, we selected a simple acyclic analog of RD of ATX (**1**, Fig. 8) as a reference compound because Kishi et al. reported that the acyclic analog of RD of ATX was capable of activating PKC.[10] The lengths of acyl and alkyl chains were set to C8, which could provide sufficient hydrophobicity to ligands as exemplified in 1,2-dioctanoyl-*sn*-glycerol (diC8), a commercially available synthetic DAG. The carbon numbering of acyclic analogs is based on those of parent compounds.

We synthesized three acyclic analogs (**1**–**3**) from known compounds **4**, **6**, and **8**, respectively (Scheme 1), and evaluated their ability to bind to the PKCδ C1B domain. In **2**, the ester group at position 27 was replaced with an ethylene group. On the other hand, in **3**, the carbonyl group at position 1 was replaced with a methylene group. In **2**, we removed both the carbonyl and the sp^3 oxygen atoms of the 27-ester group because the ring-opening of macrocycle would allow a free rotation of a C27–O27 bond, which allows the sp^3 oxygen atom to act as a hydrogen-bonding acceptor in the absence of the carbonyl group. We used the synthetic PKCδ C1B peptide[25] (δ-C1B) to precisely evaluate the affinity of ligands for the C1 domain. The concentration required to cause 50% inhibition (IC_{50}) of [^{3}H]phorbol 12,13-dibutyrate (PDBu) was measured using a competitive binding assay.[26] Affinity for δ-C1B

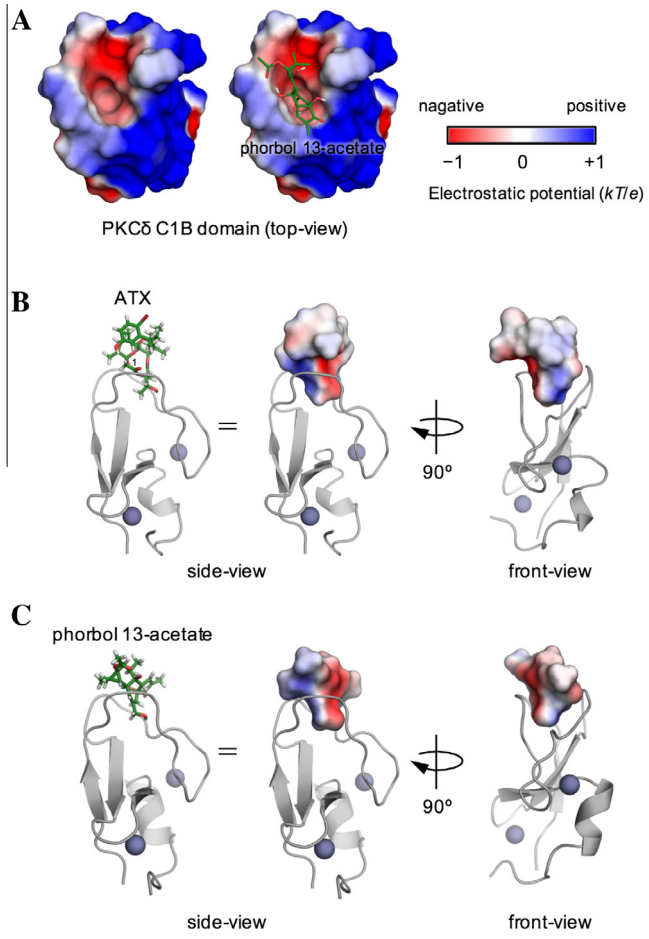

Figure 7. Molecular electrostatic potential surface representation of the PKCδ C1B domain, ATX, and phorbol 13-acetate. (A) Crystal structure of the PKCδ C1B domain (PDB code: 1PTR) in complex with phorbol 13-acetate. (B) ATX in the bound state. (C) Phorbol 13-acetate in the bound state (PDB code: 1PTR). Surfaces with negative, neutral, and positive potentials are shown in red, white, and blue, respectively.

was expressed as a K_i value calculated from the IC_{50} value of each ligand and the dissociation constant (K_d) of [^{3}H]PDBu, as reported by Goldstein and Barrett.[27]

The affinity of **3** lacking the carbonyl group at position 1 for δ-C1B (K_i, 2900 nM) was approximately eight times lower than that of **1** (K_i, 370 nM) (Table 3). On the other hand, **2** lacking the ester group at position 27 showed little binding to δ-C1B (K_i, >20,000 nM). These results suggest that the carbonyl group at position 27 was essential for receptor-recognition and the carbonyl group at position 1 also contribute to receptor recognition, which are consistent with ATX binding model from the docking simulation, the MD simulation, and the molecular electrostatic potential calculation.

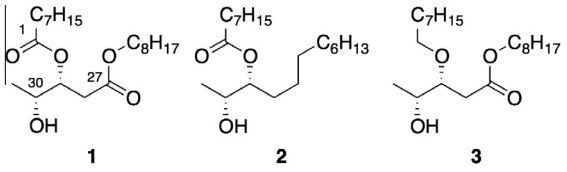

Figure 8. Structures of acyclic analogs of the recognition domain (RD) of ATX (**1**–**3**).

3. Conclusion

In conclusion, the MD simulation of the ternary complex of POPS membrane/ATX/PKCδ C1B domain suggests that the 20-OH, 27-C=O, and 30-OH groups of ATX are involved in the intermolecular hydrogen bondings, and that the ester groups at position 1 might contribute to generate molecular electrostatic potential complimentary to that of the receptor rather than hydrogen bonding. The predicted binding mode of ATX with δ-C1B was consistent with previous structure–activity studies on aplysiatoxins and provided a deeper understanding of receptor-recognition by ATX. MD simulation in explicit membrane using the binding model established in this study would be useful for the rational design of ATX derivatives as an anticancer seed with isozyme selectivity and less side effects.

4. Experimental

4.1. General remarks

The following spectroscopic and analytical instruments were used: Digital Polarimeter, Jasco P-1010 (Jasco, Tokyo, Japan); ^{1}H and ^{13}C, JOEL JNM-ECA 600 (Jeol, Japan, reference TMS); HPLC, JASCO PU-980 Intelligent HPLC pump with a JASCO PV-970 Intelligent UV/VIS Detector (JASCO, Tokyo, Japan); HR-ESI-TOF-MS, Xevo G2-XS (Waters, Tokyo, Japan). HPLC was carried out on a YMC-Pack ODS-AM AM12S05-2510WT (YMC, Kyoto, Japan). Wakogel® C-200 and C-300 (silica gel, Wako Pure Chemical Laboratory, Osaka, Japan) were used for column chromatography. [^{3}H]PDBu (17.16 Ci/mmol) was purchased from PerkinElmer Life Science Research Products (Boston, MA, US). The PKC C1 peptide was synthesized as reported previously.[25] All other chemicals and reagents were purchased from chemical companies and used without further purification.

4.2. Molecular modeling

4.2.1. Conformational search

The structures of ATX was built using Avogadro (version 1.0.3).[28] Topology of ATX for MD simulation was generated via the CGenFF server.[29] The simulated annealing was carried out using the GROMACS software package (version 5.1.2).[30] The side chain at C11 was replaced with a isopropyl group. All bonds were constrained using the LINCS algorithm. The annealing temperature was initially set to 1500 K and the temperature was kept constant for 1 ps. The temperature was linearly dropped to 100 K over 1 ps and then to 0 K over 1 ps, and kept at the same temperature for 1 ps. This 5-ps cycle was repeated 1000 times to give the conformer library. Conformers with chair–chair spiroketal conformation were selected and classified into six groups (A–F). Structures of conformers A and B were optimized using the DFT method at the level of ωB97X-D/6-31G*[31] employing Gaussian09.[32] The intermediate conformers between conformers A and B were optimized at the level of ωB97X-D/6-31G* with a dihedral restraint at C9–O9. The obtained geometries were characterized as minimum structures on the basis of their harmonic vibrational frequencies and number of imaginary frequencies.

4.2.2. Docking simulation

(a) *Protein preparation:* The crystal structure of the PKCδ C1B domain/phorbol 13-acetate complex (PDB code: 1PTR)[15] was obtained from the Protein Data Bank. (b) *Ligand preparation:* The partial atomic charge of the ligands was calculated with MOPAC2012[33] using PM6 Hamiltonian. (c) *Docking simulations:* The docking experiment was performed with AutoDock[16] 4.2.6

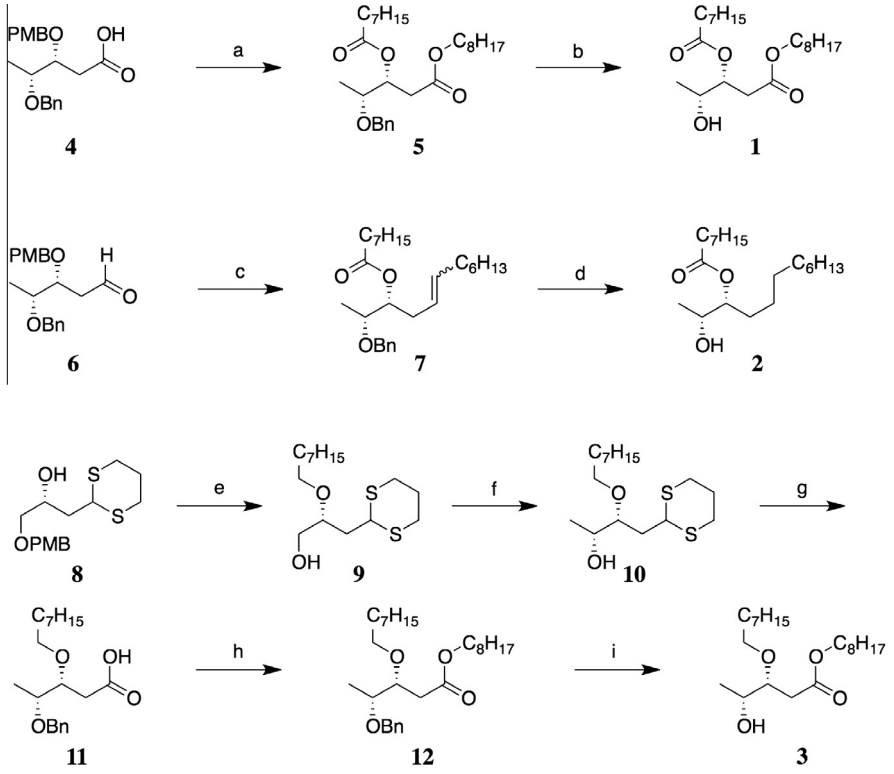

Scheme 1. Syntheses of **1**–**3**. Reagents and conditions: (a) (i) 2,4,6-trichlorobenzoyl chloride, Et_3N, *n*-octanol, DMAP, toluene; (ii) DDQ, CH_2Cl_2, H_2O, (iii) *n*-octanoyl chloride, DMAP, Et_3N, CH_2Cl_2, 34% in three steps; (b) Pd/C, H_2, EtOH, 77%; (c) (i) (1-hepthyl)triphenylphosphonium bromide, KHMDS, THF; (ii) DDQ, CH_2Cl_2, H_2O; (iii) *n*-octanoic anhydride, DMAP, pyridine, 7% in three steps; (d) Pd/C, H_2, EtOH, 65%; (e) (i) *n*-octyl bromide, NaH, DMF; (ii) DDQ, CH_2Cl_2, H_2O, 75% in two steps; (f) (i) SO_3·pyridine, Et_3N, DMSO, CH_2Cl_2; (ii) MeMgBr, $MgBr_2{\cdot}Et_2O$, CH_2Cl_2, 52% in two steps; (g) (i) BnBr, NaH, DMF; (ii) MeI, $NaHCO_3$, MeCN, H_2O; (iii) $NaClO_2$, 2-methyl-2-butene, satd NaH_2PO_4 aq, *t*-BuOH, 30% in three steps; (h) *n*-octanol, 2,4,6-trichlorobenzoyl chloride, Et_3N, DMAP, toluene, 50%; (i) Pd/C, H_2, EtOH, 85%.

Table 3
K_i values for inhibition of specific binding of [^{3}H]PDBu by **1**–**3**

Compound	K_i for δ-C1B (nM)
1	370 (280–450)[a]
2	>20,000
3	2900 (2300–3500)

[a] 95% confidence interval from at least six experiments.

and MGLTools 1.5.7 RC1. Lamarckian Genetic Algorithm was employed as the docking algorithm. A docking grid was set around the ligand-binding cleft of the receptor. (d) *Docking parameters:* Number of Genetic Algorithm (GA) runs: 200, Population size: 150, Maximum number of evaluation: 25,000,000, Maximum number of generations: 27,000.

4.2.3. MD simulation

Missing side-chains (Lys-234, Arg-274, and Glu-274) were automatically added to the crystal structure of the PKCδ C1B domain using the Swiss PDB Viewer.[34] Glycine residues were added to N- and C-termini. An initial model of POPS—ATX—PKCδ-C1B ternary complex in rectangle box filled by TIP3P water were constructed using the CHARMM-GUI[35] Bilayer Builder and the PPM Server[36] as reproducing the membrane binding model of the C1 domain calculated by Lomize et al.[37] *Z*-Length of simulation box was determined by water thickness (minimum water height on top and bottom of the system was set to 20 Å), and initial *XY*-lengths were set to 61 Å. The net charge on the system was neutralized by adding Na^+ ions. The numbers of lipid molecule in upper and lower leaflets were 64 and 58, respectively. The charmm36 force field[20] with modification for zinc-coordinated residues and the CGenFF force field were used to describe the system. Coordination of cysteine and histidine residues to zinc ions was treated as single bonds with tetrahedral geometry.

All MD simulations were performed using the GROMACS software package[30] (version 5.1.2). The geometry for the system was a rectangular box with periodic boundary conditions. The system was gradually relaxed according to CHARMM-GUI-generated position and angle restraint conditions to reach equilibrium (300 K, 1 atm). Then, 40 ns NPT (constant number of atoms, pressure, and temperature) simulation without any position restraint with 2 fs time step was performed. Production NPT simulations were performed for 10 ns with a 2 fs time step. In NPT simulation, temperature and pressure were regulated using the Nose–Hoover thermostat algorithm and the Parinello–Rahman barostat algorithm, respectively. The time constant for the temperature and pressure coupling was kept at 0.5 and 5 ps, respectively. The pressure was coupled with semi-isotropic scheme with isothermal compressibility of 4.5×10^{-5} bar^{-1}. The short-range nonbonded interactions were computed for the atom pairs within the cutoff of 1.2 nm, while the long-range electrostatic interactions were calculated using particle-mesh-Ewald summation method with fourth-order cubic interpolation and 0.16 nm grid spacing. All bonds were constrained using the parallel LINCS method. The center of mass translations of membrane, ligand/protein, and water/ion were removed every time step.

4.2.4. Molecular electrostatic potential calculation

Molecular electrostatic potentials of the PKCδ C1B domain, ATX, and phorbol 13-acetate were calculated using the APBS (Adaptive Poisson–Boltzmann Solver) program (version 1.4.2)[38] and visualized using PyMOL (version 1.7.6; Schrödinger, LLC). Molecular (sol-

vent-excluded) surface was colored by potential on solvent accessible surface. PQR files required for the calculations were generated from a GROMACS portable binary run input file (a tpr file).

4.3. Synthetic procedures

4.3.1. Synthesis of 5

To a solution of a known carboxylic acid (**4**)[39] (192.0 mg, 0.557 mmol) and Et_3N (217 μL, 1.56 mmol) in toluene (10 mL) was added 2,4,6-trichlorobenzoyl chloride (95.8 mL, 0.618 mmol) at rt under an Ar atmosphere. After 2.5 h of stirring, a supernatant of the resulting suspension was added to a solution of *n*-octanol (174 μL, 1.11 mmol) and *N*,*N*-dimethyl-4-aminopyridine (DMAP) (204.0 mg, 1.67 mmol) in toluene (10 mL) at rt. The resulting mixture was stirred for 1.5 h and then poured into water and EtOAc. The mixture was extracted with EtOAc (50 mL × 3). The combined organic layers were washed with brine, dried over Na_2SO_4, filtered, and concentrated in vacuo. The residue was purified by column chromatography (silica gel, 8% EtOAc in hexane) to afford a mixture of an octyl ester and a carboxylic acid (257.7 mg) as a colorless oil, which was taken to the next step without further purification.

To a solution of the mixture octyl ester (257.7 mg) in CH_2Cl_2 (30 mL) and H_2O (4.6 mL) was added DDQ (256.2 mg, 1.13 mmol) at rt under an Ar atmosphere. After 1 h of stirring at rt, the reaction was quenched with satd $NaHCO_3$ aq (40 mL). The resulting mixture was extracted with CH_2Cl_2 (25 mL × 3). The combined organic layers were washed with brine, dried over Na_2SO_4, filtered, and concentrated in vacuo. The residue was purified by column chromatography (silica gel, 8–15% EtOAc in hexane) to afford a mixture of an alcohol and *p*-anisaldehyde (141.0 mg) as a colorless oil, which was taken to the next step without further purification.

To a solution of the mixture alcohol (136.0 mg) and Et_3N (226 μL, 1.62 mmol) in CH_2Cl_2 (9 mL) were added *n*-octanoyl chloride (206 μL, 1.21 mmol) and DMAP (24.2 mg, 0.202 mmol) at rt under an Ar atmosphere. The resulting mixture was stirred for 2 h, and then *n*-octanoyl chloride (68.8 μL) and Et_3N (111 μL) were added. After 30 min of stirring, the reaction was quenched with H_2O (30 mL). The resulting mixture was extracted with EtOAc (30 mL × 3). The combined organic layers were washed with brine, dried over Na_2SO_4, filtered, and concentrated in vacuo. The residue was purified by column chromatography (silica gel, 2–5–15–30–50–75–100% EtOAc in hexane) to afford an octanoyl ester (92.2 mg) as a colorless oil.

A solution of the octanoyl ester (7.7 mg) in MeOH was filtered and purified by HPLC (column: YMC-Pack ODS-AM AM12S05-2510WT, solvent: 95–100% MeOH/H_2O, gradient 30 min, flow rate: 8 mL/min, UV detector: 254 nm, retention time: 19.1 min) to afford an octanoyl ester (**5**) (7.0 mg, 15.1 μmol, 49% in three steps) as a colorless oil. $[\alpha]_D$ −1.2° (*c* 0.23, $CHCl_3$, 26.4 °C). ^{1}H NMR (600 MHz, 299 K, $CDCl_3$, 9.94 mM): δ 0.88 (6H, m), 1.16 (3H, d, J = 6.4 Hz), 1.21–1.33 (18H, m), 1.60 (4H, m), 2.30 (2H, t, J = 7.6 Hz), 2.61 (1H, dd, J = 15.9, 8.6 Hz), 2.71 (1H, dd, J = 15.9, 4.8 Hz), 3.74 (1H, qd, J = 6.4, 4.0 Hz), 4.02 (2H, t, J = 6.8 Hz), 4.52 (1H, d, J = 11.9 Hz), 4.62 (1H, d, J = 11.9 Hz), 5.39 (1H, m), 7.26–7.35 (5H, m) ppm. ^{13}C NMR (150 MHz, 299 K, $CDCl_3$, 9.94 M): δ 14.1, 14.1, 14.9, 22.6, 22.6, 25.0, 25.9, 28.6, 28.9, 29.1, 29.2, 29.2, 31.7, 31.8, 34.4, 34.8, 64.9, 71.2, 71.3, 73.8, 127.7, 127.8 (2C), 128.4 (2C), 138.3, 170.8, 173.0 ppm. HR-ESI-MS: m/z = 485.3247 ([MNa]$^+$, calcd for $C_{28}H_{46}O_5Na$, 485.3243).

4.3.2. Synthesis of 1

To a solution of **5** (2.3 mg, 4.97 μmol) in EtOH (900 μL) was added Pd/C (small amount). After 20 h of stirring at rt under H_2 atmosphere, the reaction mixture was filtered, and the filtrate was concentrated in vacuo. The residue was purified by column chromatography (silica gel, 15% EtOAc in hexane) to afford **1** (1.42 mg, 3.81 μmol, 77%) as a colorless oil. $[\alpha]_D$ +9.6° (*c* 0.071, MeOH, 25.9 °C). ^{1}H NMR (600 MHz, 296 K, $CDCl_3$, 7.62 mM): δ 0.88 (6H, m), 1.20 (3H, d, J = 6.4 Hz), 1.24–1.34 (18H, m), 1.62 (4H, m), 1.87 (1H, d, J = 7.1 Hz), 2.33 (2H, m), 2.64 (1H, dd, J = 15.8, 7.6 Hz), 2.72 (1H, dd, J = 15.8, 5.6 Hz), 3.93 (1H, m), 4.06 (2H, t, J = 6.8 Hz), 5.16 (1H, m) ppm. ^{13}C NMR (150 MHz, 296 K, $CDCl_3$, 7.62 mM): δ 14.1, 14.1, 19.3, 22.6, 22.6, 25.0, 25.9, 28.6, 28.9, 29.1, 29.2, 29.2, 31.7, 31.8, 34.3, 35.8, 65.1, 68.3, 73.3, 170.7, 173.2 ppm. HR-ESI-MS: m/z = 395.2773 ([MNa]$^+$, calcd for $C_{21}H_{40}O_5Na$, 395.2773).

4.3.3. Synthesis of 7

To a suspension of heptyltriphenylphosphonium bromide (107.7 mg, 0.244 mmol) in THF (1.5 mL) was added a 0.5 M solution of KHMDS in toluene (390 μL, 0.195 mmol) at −78 °C under an Ar atmosphere. The resulting mixture was stirred at rt for 40 min. The reaction mixture was recooled to −78 °C, and then a solution of a known aldehyde (**6**)[40] (40.1 mg, 0.122 mmol) in THF (800 μL) was added. After 18 h of stirring at rt, the reaction was quenched with H_2O (1.5 mL), and then was extracted with EtOAc (6 mL × 3). The combined organic layers were washed with brine, dried over Na_2SO_4, filtered, and concentrated in vacuo. The residue was purified by column chromatography (silica gel, 10–20% EtOAc in hexane) to afford a mixture of an olefin and the by-product (24.0 mg), which was taken to the next step without further purification.

To a solution of the mixture olefin (24.0 mg) in CH_2Cl_2 (3.1 mL) and H_2O (480 μL) was added DDQ (19.9 mg, 0.876 mmol) at rt. The reaction mixture was stirred for 3 h, and then DDQ (19.9 mg, 0.876 mmol) was added. After 1 h of stirring, the reaction was quenched with satd $NaHCO_3$ aq (10 mL). The resulting mixture was extracted with CH_2Cl_2 (15 mL × 3). The combined organic layers were washed with brine, dried over Na_2SO_4, filtered, and concentrated in vacuo. The residue was purified by column chromatography (silica gel, 10% EtOAc in hexane) to afford a mixture of an alcohol and *p*-anisaldehyde (4.6 mg) as a pale yellow oil, which was taken to the next step without further purification.

To a solution of the mixture alcohol (4.6 mg) in pyridine (300 μL) were added octanoic anhydride (5.7 μL, 19.2 μmol) and DMAP (small amount) at rt under an Ar atmosphere. After 3 h of stirring, the reaction was quenched with H_2O (300 μL). The resulting mixture was extracted with EtOAc (3 mL × 3). The combined organic layers were washed with 5% (*w*/*v*) $NaHCO_3$ aq and brine, dried over Na_2SO_4, filtered, and concentrated in vacuo. The residue was purified by column chromatography (silica gel, 5% EtOAc in hexane) to afford an octanoyl ester as a colorless oil. A solution of the octanoyl ester in MeOH was filtered and purified by HPLC (column: YMC-Pack ODS-AM AM12S05-2510WT, solvent: 95% MeOH/H_2O, flow rate: 8 mL/min, UV detector: 254 nm, retention time: 26.8 min) to afford the octanoyl ester (**7**) (3.6 mg, 8.64 μmol, 7% in three steps) as a colorless oil. $[\alpha]_D$ −11.8° (*c* 0.507, MeOH, 26.8 °C). ^{1}H NMR (600 MHz, 296 K, $CDCl_3$, 0.0173 M): δ 0.87 (3H, t, J = 7.1 Hz), 0.88 (3H, t, J = 7.0 Hz), 1.16 (3H, d, J = 6.4 Hz), 1.21–1.36 (16H, m), 1.61 (2H, m), 2.02 (2H, br q, J = 6.9 Hz), 2.30 (2H, t, J = 7.6 Hz), 2.37 (2H, t, J = 7.2 Hz), 3.64 (1H, m), 4.51 (1H, d, J = 12.0 Hz), 4.63 (1H, d, J = 12.0 Hz), 4.97 (1H, m), 5.28 (1H, m), 5.45 (1H, m), 7.26–7.43 (5H, m) ppm. ^{13}C NMR (150 MHz, 296 K, $CDCl_3$, 0.0173 M): δ 14.1, 14.1, 15.4, 22.6, 22.6, 25.1, 27.4, 27.8, 29.0, 29.0, 29.1, 29.6, 31.7, 31.8, 34.5, 71.2, 74.5, 75.2, 124.3, 127.5, 127.6 (2C), 128.3 (2C), 132.8, 138.6, 173.6 ppm. HR-ESI-MS: m/z = 439.3187 ([MNa]$^+$, calcd for $C_{27}H_{44}O_3Na$, 439.3188).

4.3.4. Synthesis of 2

To a solution of **7** (3.6 mg, 8.64 μmol) in EtOH (700 μL) was added Pd/C (small amount). After 4 h of stirring under a H_2 atmosphere, the reaction mixture was filtered, and the filtrate was

concentrated in vacuo. The residue was purified by column chromatography (silica gel, 10% EtOAc in hexane) to afford **2** (1.84 mg, 5.60 μmol, 65%) as colorless oil. $[\alpha]_D$ +9.6° (*c* 0.0920, MeOH, 20.2 °C). ^{1}H NMR (600 MHz, 296 K, $CDCl_3$, 0.0184 M): δ 0.88 (6H, m), 1.17 (3H, d, *J* = 6.4 Hz), 1.22–1.33 (22H, m), 1.59 (2H, m), 1.64 (2H, m), 1.68 (1H, br d, *J* = 6.9 Hz), 2.35 (2H, t, *J* = 7.6 Hz), 3.80 (1H, m), 4.78 (1H, dt, *J* = 7.9, 5.0 Hz) ppm. ^{13}C NMR (150 MHz, 296 K, $CDCl_3$, 0.0184 M): δ 14.1, 14.1, 19.7, 22.6, 22.7, 25.2, 25.3, 29.1, 29.0, 29.3, 29.5 (3C), 30.6, 31.7, 31.9, 34.5, 68.8, 77.5, 173.9 ppm. HR-ESI-MS: *m*/*z* = 351.2862 ([MNa]$^+$, calcd for $C_{20}H_{40}O_3Na$, 351.2852).

4.3.5. Synthesis of 9

To a suspension of 60% NaH in oil (382.0 mg, 9.55 mmol) in DMF (10 mL) was added a solution of a known alcohol (**8**)[39] (1201.3 mg, 3.82 mmol) in DMF (24 mL). After 30 min of stirring at 0 °C, 1-bromooctane (1.3 mL, 7.6 mmol) was added dropwise. The mixture was stirred for 30 min, and then warmed to rt. After 3.5 h of stirring, the reaction was quenched with H_2O (25 mL), and the resulting mixture was diluted with EtOAc (25 mL). The organic layer was separated, and the aqueous layer was extracted with EtOAc (50 mL × 3). The combined organic layers were washed with brine, dried over Na_2SO_4, filtered, and concentrated in vacuo. The residue was purified by column chromatography (silica gel, 7% EtOAc in hexane) to afford a mixture of an octyl ether and an alcohol (1.477 mg) as a colorless oil, which was taken to the next step without further purification.

To a solution of the mixture octyl ether (1307 mg) in CH_2Cl_2 (162 mL) and H_2O (24.8 mL) was added DDQ (1.4 g, 6.1 mmol) at rt. After 1.5 h of stirring, the reaction was quenched with satd $NaHCO_3$ aq (160 mL). The resulting mixture was extracted with CH_2Cl_2 (150 mL × 3). The combined organic layers were washed with brine, dried over Na_2SO_4, filtered, and concentrated in vacuo. The residue was purified by column chromatography (silica gel, 15–30% EtOAc in hexane) to afford an alcohol (**9**) (778.8 mg, 2.54 mmol, 75% in two steps) as a colorless oil. $[\alpha]_D$ −3.6° (*c* 1.00, $CHCl_3$, 26.1 °C). ^{1}H NMR (600 MHz, 300 K, $CDCl_3$, 0.0568 M): δ 0.88 (3H, t, *J* = 7.0 Hz), 1.27–1.39 (10H, m), 1.54–1.61 (2H, m), 1.83–1.94 (3H, m), 2.05 (1H, m), 2.12 (1H, m), 2.81–2.95 (4H, m), 3.47–3.57 (3H, m), 3.64–3.68 (1H, m), 3.75 (1H, dt, *J* = 11.4, 4.2 Hz), 4.14 (1H, m) ppm. ^{13}C NMR (150 MHz, 300 K, $CDCl_3$, 0.0568 M): δ 14.1, 22.7, 25.9, 26.2, 29.3, 29.4, 30.1 (2C), 30.4, 31.9, 37.2, 43.8, 63.9, 70.1, 76.2 ppm. HR-ESI-MS: *m*/*z* = 329.1580 ([MNa]$^+$, calcd for $C_{15}H_{30}O_2NaS_2$, 329.1585).

4.3.6. Synthesis of 10

To a solution of **9** (178.6 mg, 0.583 mmol) in CH_2Cl_2 (2.4 mL) and DMSO (611 μL) were added Et_3N (568 μL, 4.08 mmol) and SO_3·pyridine (370.8 mg, 2.33 mmol) at 0 °C. After 2.5 h of stirring at rt, the reaction was quenched with satd NH_4Cl aq (5 mL). The resulting mixture was extracted with CH_2Cl_2 (10 mL × 3). The combined organic layers were washed with brine, dried over Na_2SO_4, filtered, and concentrated in vacuo. The residue was purified by column chromatography (silica gel, 7–10% EtOAc in hexane) to afford a mixture of an aldehyde and the by-product (120.1 mg) as a pale yellow oil, which was taken to the next step without further purification.

To a solution of the mixture aldehyde (12.1 mg) in CH_2Cl_2 (300 μL) was added $MgBr_2$·Et_2O (12.3 mg, 47.6 μmol) at −78 °C. The mixture was stirred for 1 h, and then 3 M CH_3MgBr in diethyl ether (199 μL, 59.6 μmol) was added dropwise at −78 °C. After 1.5 h of stirring, the reaction was quenched with satd NH_4Cl aq (2 mL). The resulting mixture was extracted with CH_2Cl_2 (10 mL × 3). The combined organic layers were washed with brine, dried over Na_2SO_4, filtered, and concentrated in vacuo. The residue was purified by column chromatography (silica gel, 15% EtOAc in hexane) to afford an alcohol (**10**) (9.9 mg, 30.9 μmol, 52% in two steps) as a pale yellow oil. $[\alpha]_D$ +1.9° (*c* 0.97, $CHCl_3$, 26.3 °C). ^{1}H NMR (600 MHz, 298 K, $CDCl_3$, 0.0618 M): δ 0.88 (3H, t, *J* = 7.1 Hz), 1.20 (3H, d, *J* = 6.4 Hz), 1.25–1.40 (10H, m), 1.55–1.61 (2H, m), 1.84–1.90 (1H, m), 1.90–1.96 (2H, m), 2.09–2.26 (1H, m), 2.22 (1H, d, *J* = 5.0 Hz), 2.78–2.95 (4H, m), 3.38 (1H, dd, *J* = 12.0, 5.5 Hz), 3.54 (1H, dt, *J* = 9.1, 6.6 Hz), 3.66 (1H, m), 3.71 (1H, m), 4.15 (1H, *J* = 7.3 Hz) ppm. ^{13}C NMR (150 MHz, 298 K, $CDCl_3$, 0.0618 M): δ 14.1, 19.3, 22.7, 25.9, 26.2, 29.3, 29.5, 30.2, 30.3, 30.5, 31.8, 37.2, 43.9, 69.4, 71.8, 80.3 ppm. HR-ESI-MS: *m*/*z* = 343.1733 ([MNa]$^+$, calcd for $C_{16}H_{32}O_2NaS_2$, 343.1741).

4.3.7. Synthesis of 11

To a suspension of 60% NaH in oil (103.2 mg, 2.58 mmol) in DMF (5 mL) was added a solution of **10** (413.5 mg, 1.29 mmol) in DMF (10 mL) at 0 °C. After 30 min of stirring, BnBr (230 μL, 1.94 mmol) was added dropwise. The reaction mixture was stirred for 30 min, and then warmed to rt. After 4 h of stirring, the reaction was quenched with satd NH_4Cl aq (12 mL). The resulting mixture was extracted with EtOAc (20 mL × 3). The combined mixture was washed with brine, dried over Na_2SO_4, filtered, and concentrated in vacuo. The residue was purified by column chromatography (silica gel, 2–10–15% EtOAc in hexane) to afford a mixture of a benzyl ether and a reagent (252.0 mg) as a colorless oil and a recovered substrate (235.1 mg, 0.733 mmol, 57%). The benzyl ether mixture was taken to the next step without further purification.

To a solution of the mixture benzyl ether (235.1 mg) in CH_3CN (5.3 mL) and H_2O (1.3 mL) were added $NaHCO_3$ (142 mg, 1.69 mmol) and CH_3I (1.4 mL, 22.5 mmol) at rt. After 18 h of stirring, the reaction mixture was extracted with EtOAc (10 mL × 3). The combined organic layers were washed with brine, dried over Na_2SO_4, filtered, and concentrated in vacuo. The residue was purified by column chromatography (silica gel, 5–15% EtOAc in hexane) to afford a mixture of an aldehyde and the by-product (149.0 mg) as a colorless oil, which was taken to the next step without purification.

To a solution of the mixture of the aldehyde (117.6 mg) in *t*-BuOH (2.9 mL) and satd NaH_2PO_4 aq (1.5 mL) was added a solution of 2-methyl-2-butene (276 μL) and $NaClO_2$ (66.2 mg, 0.512 mmol) in satd NaH_2PO_4 aq (1.4 mL) at 0 °C. After 10 min of stirring, the reaction was quenched with 5% H_3PO_4 aq (7 mL). The resulting mixture was extracted with EtOAc (7 mL × 3). The combined organic layers were washed with brine, dried over Na_2SO_4, filtered, and concentrated in vacuo. The residue was purified by column chromatography (silica gel, 100% $CHCl_3$) to afford a carboxylic acid (**11**) (121.7 mg, 0.367 mmol, 30% in three steps) as a colorless oil. $[\alpha]_D$ −0.4° (*c* 0.67, $CHCl_3$, 26.4 °C). ^{1}H NMR (600 MHz, 300 K, $CDCl_3$, 0.0297 M): δ 0.88 (3H, m), 1.17 (3H, d, *J* = 6.4 Hz), 1.21–1.30 (10H, m), 1.52 (2H, m), 2.49 (1H, dd, *J* = 15.8, 8.1 Hz), 2.68 (1H, dd, *J* = 15.8, 4.3 Hz), 3.52 (2H, t, *J* = 6.6 Hz), 3.70 (1H, m), 3.84 (1H, m), 4.51 (1H, d, *J* = 11.9 Hz), 4.61 (1H, d, *J* = 11.9 Hz), 7.26–7.35 (5H, m) ppm. ^{13}C NMR (150 MHz, 300 K, $CDCl_3$, 0.0297 M): δ 14.1, 14.4, 22.7, 26.1, 29.3, 29.4, 30.0, 31.8, 35.1, 71.1, 71.2, 74.6, 77.7, 127.6, 127.7 (2C), 128.4 (2C), 138.4, 176.3 ppm. HR-ESI-MS: *m*/*z* = 359.2190 ([MNa]$^+$, calcd for $C_{20}H_{32}O_4Na$, 359.2198).

4.3.8. Synthesis of 12

To a solution of **11** (57.2 mg, 0.170 mmol) and Et_3N (66.3 μL, 0.476 mmol) in toluene (3 mL) was added 2,4,6-trichlorobenzoyl chloride (29.1 μL, 0.187 mmol) at rt. After 2.5 h of stirring, a supernatant of the resulting suspension was added to a solution of *n*-octanol (53.3 μL, 0.34 mmol) and DMAP (62.3 mg, 0.51 mmol) in toluene (10 mL) at rt. The resulting mixture was stirred for 1.5 h and then poured into water and EtOAc. The mixture was extracted with EtOAc (15 mL × 3). The combined organic layers were washed with brine, dried over Na_2SO_4, filtered, and concentrated in vacuo.

The residue was purified by column chromatography (silica gel, 3% EtOAc in hexane) to afford a mixture of an octyl ester and 2,4,6-trichlorobenzoic acid. The mixture was further purified by column chromatography (silica gel, 1–2% EtOAc in hexane) to afford a mixture of the ester and the carboxylic acid (85.8 mg), and a pure ester (44.1 mg) as a colorless oil, respectively. A pure portion of the ester (11.0 mg) was purified by HPLC (column: YMC-Pack ODS-AM AM12S05-2510WT, solvent: a linear gradient of 95–100% MeOH/H_2O over 30 min, flow rate: 8 mL/min, UV detector: 254 nm, retention time: 22.5 min) to afford an octanoyl ester (**12**) (9.6 mg, 21.3 μmol, 50%) as a colorless oil. $[\alpha]_D$ +1.2° (*c* 0.37, $CHCl_3$, 26.6 °C). ^1H NMR (600 MHz, 300 K, $CDCl_3$, 0.0165 M): δ 0.88 (6H, m), 1.16 (3H, d, J = 6.4 Hz), 1.22–1.36 (20H, m), 1.50 (2H, m), 1.61 (2H, m), 2.45 (1H, dd, J = 15.5, 8.8 Hz), 2.59 (1H, dd, J = 15.5, 4.1 Hz), 3.49 (2H, m), 3.68 (1H, m), 3.88 (1H, quint, J = 4.3 Hz), 4.05 (2H, m), 4.52 (1H, d, J = 11.8 Hz), 4.66 (1H, d, J = 11.8 Hz), 7.26–7.33 (5H, m) ppm. ^{13}C NMR (150 MHz, 300 K, $CDCl_3$, 0.0165 M): δ 14.1 (2C), 14.5, 22.7 (2C), 26.0, 26.1, 28.7, 29.2, 29.3, 29.3, 29.5, 30.1, 31.8, 31.9, 35.6, 64.7, 71.1, 71.2, 74.8, 78.0, 127.5, 127.7 (2C), 128.3 (2C), 138.7, 172.4 ppm. HR-ESI-MS: m/z = 471.3454 ([MNa]$^+$, calcd for $C_{28}H_{48}O_4Na$, 471.3450).

4.3.9. Synthesis of 3

To a solution of **12** (13.3 mg, 29.6 μmol) in EtOH (1.5 mL) was added Pd/C (1.3 mg) at rt. After 21 h of stirring under a H_2 atmosphere, the reaction mixture was filtered. The filtrate was purified by column chromatography (silica gel, 5–8% EtOAc in hexane) to afford 3 (9.04 mg, 25.2 μmol, 85%) as a colorless oil. $[\alpha]_D$ +4.9° (*c* 0.452, MeOH, 19.4 °C) ^1H NMR (600 MHz, 295 K, $CDCl_3$, 0.0428 M): δ 0.88 (6H, t, J = 7.0 Hz), 1.20 (3H, d, J = 6.4 Hz), 1.26–1.35 (20H, m), 1.51–1.66 (4H, m), 2.35 (1H, s), 2.51 (1H, dd, J = 15.5, 6.4 Hz), 2.55 (1H, dd, J = 15.6, 5.5 Hz), 3.46 (1H, dt, J = 9.0, 6.7 Hz), 3.55 (1H, m), 3.61 (1H, m), 3.72 (1H, quintet, J = 6.0 Hz), 4.09 (2H, m) ppm. ^{13}C NMR (150 MHz, 295 K, $CDCl_3$, 0.0428 M): δ 14.1 (2C), 18.9, 22.6 (2C), 25.9, 26.1, 28.6, 29.2, 29.2, 29.3, 29.4, 30.1, 31.8, 31.8, 36.5, 64.9, 69.4, 71.2, 80.4, 171.8 ppm. HR-ESI-MS: m/z = 381.2980 ([MNa]$^+$, calcd for $C_{21}H_{42}O_4Na$, 381.2981).

4.4. Inhibition of specific binding of [^{3}H]PDBu to the PKCδ C1B peptide

The binding of [^{3}H]PDBu to the PKCδ C1B peptide was evaluated by the procedure of Sharkey and Blumberg[27] with modifications as reported previously[41] using 50 mM Tris–maleate buffer (pH 7.4 at 4 °C), 13.8 nM PKCδ C1B peptide, 5 (for **2** and **3**) or 20 (for **1**) nM [^{3}H]PDBu (17.16 Ci/mmol, Perkin–Elmer Life Science), 50 μg/mL 1,2-dioleoyl-*sn*-glycero-3-phospho-L-serine (Funakoshi), 3 mg/mL bovine γ-globulin (Sigma), and various concentrations of inhibitors. Binding affinity was evaluated on the basis of the concentration required to cause 50% inhibition of the specific binding of [^{3}H]PDBu, IC_{50}, which was calculated by logit analysis using Microsoft Excel. When the inhibition rate of specific binding of [^{3}H]PDBu did not fall below 50%, IC_{50} was extrapolated from regression line. The binding inhibition constant, K_i, was calculated by the formula of Goldstein and Barrett,[28] $K_i = IC_{50}/(2[L_{50}]/[L_0] - 1 + [L_{50}]/K_d)$, where $[L_{50}]$ and $[L_0]$ are the free concentration of [^{3}H]PDBu at 50% and 0% inhibition, respectively. Although we used PKCδ C1B peptide in 13.8 nM, the concentration of the properly folded peptide was estimated to be about 3–4 nM on the base of B_{max} value of Scatchard analysis reported previously.[40] Therefore, the concentration of free PDBu did not markedly vary over the dose–response curve.

Acknowledgements

This work was supported by a Grant-in-Aid for Scientific Research on Innovative Areas 'Chemical Biology of Natural Products' [number 23102011] (to K.I. and R.C.Y.) from The Ministry of Education, Culture, Sports, Science, and Technology, Japan.

The docking and MD simulations were carried out at the Research Center for Computational Science, Okazaki Research Facilities, National Institutes of Natural Sciences (NINS).

Supplementary data

Supplementary data (root mean square deviation (RMSD) of the PKCδ C1B domain and ATX during MD simulation. NMR spectra of **1**–**3**) associated with this article can be found, in the online version, at http://dx.doi.org/10.1016/j.bmc.2016.07.011.

References and notes

1. Kato, Y.; Scheuer, P. J. *J. Am. Chem. Soc.* **1974**, *96*, 2245.
2. Moore, R. E. *Pure Appl. Chem.* **1982**, *54*, 1919.
3. Fujiki, H.; Sugimura, T. *Adv. Cancer Res.* **1987**, *49*, 223.
4. Ramos, O. F.; Masucci, M. G.; Klein, E. *Cancer Res.* **1984**, *44*, 1857.
5. Nishizuka, Y. *Nature* **1984**, *308*, 693.
6. Mackay, H. J.; Twelves, C. J. *Nat. Rev. Cancer* **2007**, *7*, 554.
7. Arcoleo, J. P.; Weinstein, I. B. *Carcinogenesis* **1985**, *6*, 213.
8. Nakagawa, Y.; Yanagita, R. C.; Hamada, N.; Murakami, A.; Takahashi, H.; Saito, N.; Nagai, H.; Irie, K. *J. Am. Chem. Soc.* **2009**, *131*, 7573.
9. Irie, K.; Yanagita, R. C. *Chem. Rec.* **2014**, *14*, 251.
10. Kong, F.; Kishi, Y.; Perez-Sala, D.; Rando, R. R. *Proc. Natl. Acad. Sci. U.S.A.* **1991**, *88*, 1973.
11. Nakamura, H.; Kishi, Y.; Pajares, M. A.; Rando, R. R. *Proc. Natl. Acad. Sci. U.S.A.* **1989**, *86*, 9672.
12. Giorgione, J. R.; Lin, J. H.; McCammon, J. A.; Newton, A. C. *J. Biol. Chem.* **2006**, *281*, 1660.
13. (a) Knust, H.; Hoffmann, R. W. *Chem. Rec.* **2002**, *2*, 405; (b) Knust, H.; Hoffmann, R. W. *Helv. Chim. Acta* **2003**, *86*, 1871.
14. Moore, R. E.; Blackman, A. J.; Cheuk, C. E.; Mynderse, J. S.; Matsumoto, G. K.; Clardy, J.; Woodard, R. W.; Craig, J. C. *J. Org. Chem.* **1984**, *49*, 2484.
15. Zhang, G.; Kazanietz, M. G.; Blumberg, P. M.; Hurley, J. H. *Cell* **1995**, *81*, 917.
16. Morris, G. M.; Huey, R.; Lindstrom, W.; Sanner, M. F.; Belew, R. K.; Goodsell, D. S.; Olson, A. J. *J. Comput. Chem.* **2009**, *30*, 2785.
17. Sigano, D. M.; Peach, M. L.; Nacro, K.; Choi, Y.; Lewin, N. E.; Nicklaus, M. C.; Blumberg, P. M.; Marquez, V. E. *J. Med. Chem.* **2003**, *46*, 1571.
18. Li, J.; Ziemba, B. P.; Falke, J. J.; Voth, G. A. *J. Am. Chem. Soc.* **2014**, *136*, 11757.
19. Dries, D. R.; Gallegos, L. L.; Newton, A. C. *J. Biol. Chem.* **2007**, *282*, 826.
20. (a) Best, R. B.; Zhu, X.; Shim, J.; Lopes, P. E.; Mittal, J.; Feig, M.; MacKerell, A. D., Jr. *J. Chem. Theory Comput.* **2012**, *8*, 3257; (b) Klauda, J. B.; Venable, R. M.; Freites, J. A.; O'Connor, J. W.; Tobias, D. J.; Mondragon-Ramirez, C.; Vorobyov, I.; MacKerell, A. D., Jr.; Pastor, R. W. *J. Phys. Chem. B* **2010**, *114*, 7830.
21. Suganuma, M.; Fujiki, H.; Tahira, T.; Cheuk, C.; Moore, R. E.; Sugimura, T. *Carcinogenesis* **1984**, *5*, 315.
22. Keck, G. E.; Poudel, Y. B.; Rudra, A.; Stephens, J. C.; Kedei, N.; Lewin, N. E.; Peach, M. L.; Blumberg, P. M. *Angew. Chem., Int. Ed.* **2010**, *49*, 4580.
23. Jeffrey, George A. *An Introduction to Hydrogen Bonding*; Oxford University Press: Oxford, 1997.
24. Náray-Szabó, G. *J. Mol. Recognit.* **1993**, *6*, 205.
25. Irie, K.; Oie, K.; Nakahara, A.; Yanai, Y.; Ohigashi, H.; Wender, P. A.; Fukuda, H.; Konishi, H.; Kikkawa, U. *J. Am. Chem. Soc.* **1998**, *120*, 9159.
26. Sharkey, N. A.; Blumberg, P. M. *Cancer Res.* **1985**, *45*, 19.
27. Goldstein, A.; Barrett, R. W. *Mol. Pharmacol.* **1987**, *31*, 603.
28. Hanwell, M. D.; Curtis, D. E.; Lonie, D. C.; Vandermeersch, T.; Zurek, E.; Hutchison, G. R. *J. Cheminform.* **2012**, *4*, 17.
29. Vanommeslaeghe, K.; Hatcher, E.; Acharya, C.; Kundu, S.; Zhong, S.; Shim, J.; Darian, E.; Guvench, O.; Lopes, P.; Vorobyov, I.; MacKerell, A. D., Jr. *J. Comput. Chem.* **2010**, *31*, 671.
30. van der Spoel, D.; Lindahl, E.; Hess, B.; Groenhof, G.; Mark, A. E.; Berendsen, H. J. C. *J. Comput. Chem.* **2005**, *26*, 1701.
31. Chai, J. D.; Head-Gordon, M. *Phys. Chem. Chem. Phys.* **2008**, *10*, 6615.
32. Frisch, M. J.; Trucks, G. W.; Schlegel, H. B.; Scuseria, G. E.; Robb, M. A.; Cheeseman, J. R.; Scalmani, G.; Barone, V.; Mennucci, B.; Petersson, G. A.; Nakatsuji, H.; Caricato, M.; Li, X.; Hratchian, H. P.; Izmaylov, A. F.; Bloino, J.; Zheng, G.; Sonnenberg, J. L.; Hada, M.; Ehara, M.; Toyota, K.; Fukuda, R.; Hasegawa, J.; Ishida, M.; Nakajima, T.; Honda, Y.; Kitao, O.; Nakai, H.; Vreven, T., ; Montgomery, J. A., Jr.; Peralta, J. E.; Ogliaro, F.; Bearpark, M.; Heyd, J. J.; Brothers, E.; Kudin, K. N.; Staroverov, V. N.; Kobayashi, R.; Normand, J.; Raghavachari, K.; Rendell, A.; Burant, J. C.; Iyengar, S. S.; Tomasi, J.; Cossi, M.; Rega, N.; Millam, J. M.; Klene, M.; Knox, J. E.; Cross, J. B.; Bakken, V.; Adamo, C.; Jaramillo, J.; Gomperts, R.; Stratmann, R. E.; Yazyev, O.; Austin, A. J.; Cammi, R.; Pomelli, C.; Ochterski, J. W.; Martin, R. L.; Morokuma, K.; Zakrzewski, V. G.; Voth, G. A.; Salvador, P.; Dannenberg, J. J.; Dapprich, S.; Daniels, A. D.; Farkas, Ö.; Foresman, J. B.; Ortiz, J. V.; Cioslowski, J.; Fox, D. J. *Gaussian 09. Revision D.01*; Gaussian: Wallingford CT, 2009.
33. MOPAC2012, Stewart, J. J. P.; Stewart Computational Chemistry; Colorado Springs: CO, USA, 2012. http://OpenMOPAC.net.

34. Guex, N.; Peitsch, M. C. *Electrophoresis* **1997**, *18*, 2714.
35. Jo, S.; Kim, T.; Iyer, V. G.; Im, W. *J. Comput. Chem.* **2008**, *29*, 1859.
36. Lomize, M. A.; Pogozheva, I. D.; Joo, H.; Mosberg, H. I.; Lomize, A. L. *Nucleic Acids Res.* **2012**, *40*, D370.
37. Lomize, A. L.; Pogozheva, I. D.; Lomize, M. A.; Mosberg, H. I. *BMC Struct. Biol.* **2007**, *7*, 44.
38. Baker, N. A.; Sept, D.; Joseph, S.; Holst, M. J.; McCammon, J. A. *Porc. Natl. Acad. Sci. U.S.A.* **2001**, *98*, 10037.
39. Hanaki, Y.; Kikumori, M.; Ueno, S.; Tokuda, H.; Suzuki, N.; Irie, K. *Tetrahedron* **2013**, *69*, 7636.
40. Wender, P. A.; Brabander, J. D.; Harran, P. G.; Jimenez, J. M.; Koehler, M. F. T.; Lippa, B.; Park, C. M.; Shiozaki, M. *J. Am. Chem. Soc.* **1998**, *120*, 4534.
41. Shindo, M.; Irie, K.; Nakahara, A.; Ohigashi, H.; Konishi, H.; Kikkawa, U.; Fukuda, H.; Wender, P. A. *Bioorg. Med. Chem.* **2001**, *9*, 2073.

Please cite this article in press as: Ashida, Y.; et al. *Bioorg. Med. Chem.* (2016), http://dx.doi.org/10.1016/j.bmc.2016.07.011